UC San Diego
UC San Diego Previously Published Works

Title

Three-dimensional ultrashort echo time cones T1ρ (3D UTE-cones-T1ρ) imaging

Permalink

Journal

ISSN

Authors

Ma, Ya-Jun
Carl, Michael
Shao, Hongda
et al.

Publication Date

DOI

Copyright Information

Peer reviewed

WILEY **NMR** IN BIOMEDICINE

RESEARCH ARTICLE

Three-dimensional ultrashort echo time cones $T_{1\rho}$ (3D UTE-cones-$T_{1\rho}$) imaging

Ya-Jun Ma[1] | Michael Carl[2] | Hongda Shao[1,3] | Anthony S. Tadros[1] | Eric Y. Chang[1,4] | Jiang Du[1] (iD)

[1] Department of Radiology, University of California, San Diego, CA, USA

[2] GE Healthcare, San Diego, CA, USA

[3] Department of Radiology, Shanghai Tenth People's Hospital, Tongji University School of Medicine, Shanghai, China

[4] Radiology Service, VA San Diego Healthcare System, San Diego, CA, USA

Correspondence
J. Du, Department of Radiology, University of California, 200 West Arbor Drive, San Diego, CA 92103-8226, USA
Email: jiangdu@ucsd.edu.

Funding information
National Institutes of Health, Grant/Award Number: 1 R01 AR068987-01.

We report a novel three-dimensional (3D) ultrashort echo time (UTE) sequence employing Cones trajectory and $T_{1\rho}$ preparation (UTE-Cones-$T_{1\rho}$) for quantitative $T_{1\rho}$ assessment of short T_2 tissues in the musculoskeletal system. A basic 3D UTE-Cones sequence was combined with a spin-locking preparation pulse for $T_{1\rho}$ contrast. A relatively short TR was used to decrease the scan time, which required T_1 measurement and compensation using 3D UTE-Cones data acquisitions with variable TRs. Another strategy to reduce the total scan time was to acquire multiple Cones spokes (N_{sp}) after each $T_{1\rho}$ preparation and fat saturation. Four spin-locking times (TSL = 0–20 ms) were acquired over 12 min, plus another 7 min for T_1 measurement. The 3D UTE-Cones-$T_{1\rho}$ sequence was compared with a two-dimensional (2D) spiral-$T_{1\rho}$ sequence for the imaging of a spherical $CuSO_4$ phantom and *ex vivo* meniscus and tendon specimens, as well as the knee and ankle joints of healthy volunteers, using a clinical 3-T scanner. The $CuSO_4$ phantom showed a $T_{1\rho}$ value of 76.5 ± 1.6 ms with the 2D spiral-$T_{1\rho}$ sequence, as well as 85.7 ± 3.6 and 89.2 ± 1.4 ms for the 3D UTE-Cones-$T_{1\rho}$ sequences with N_{sp} of 1 and 5, respectively. The 3D UTE-Cones-$T_{1\rho}$ sequence provided shorter $T_{1\rho}$ values for the bovine meniscus sample relative to the 2D spiral-$T_{1\rho}$ sequence (10–12 ms *versus* 16 ms, respectively). The cadaveric human Achilles tendon sample could only be imaged with the 3D UTE-Cones-$T_{1\rho}$ sequence ($T_{1\rho} = 4.0 \pm 0.9$ ms), with the 2D spiral-$T_{1\rho}$ sequence demonstrating near-zero signal intensity. Human studies yielded $T_{1\rho}$ values of 36.1 ± 2.9, 18.3 ± 3.9 and 3.1 ± 0.4 ms for articular cartilage, meniscus and the Achilles tendon, respectively. The 3D UTE-Cones-$T_{1\rho}$ sequence allows volumetric $T_{1\rho}$ measurement of short T_2 tissues *in vivo*.

KEYWORDS

Cones, meniscus, short T_2, T_1, $T_{1\rho}$, tendon, UTE

1 | INTRODUCTION

Osteoarthritis (OA) affects millions of people and has a substantial impact on the economy and the healthcare system worldwide. Amongst the most significant early changes in OA is the loss of proteoglycans (PGs) in articular cartilage.[1] Although delayed gadolinium-

enhanced magnetic resonance imaging (MRI) of cartilage (dGEMRIC) and sodium imaging have been used previously to measure PG distribution,[2,3] spin–lattice relaxation in the rotating frame ($T_{1\rho}$) has been proposed as an attractive alternative to probe biochemical changes in cartilage.[4–6] $T_{1\rho}$ reflects the slow interactions between motion-restricted water molecules and their local macromolecular environment, and provides unique biochemical information in the low-frequency region, ranging from a few hundred hertz to a few kilohertz.[7] Changes to the extracellular matrix (ECM), such as PG loss, may be reflected in measurements of $T_{1\rho}$ and $T_{1\rho}$ dispersion ($T_{1\rho}$ values as a function of the spin-locking field). Recent studies have demonstrated that $T_{1\rho}$ shows high sensitivity to PG loss in suspensions and bovine cartilage samples, as well as in patients with OA.[4–6,8,9]

Abbreviations used: 2D, two-dimensional; 3D, three-dimensional; dGEMRIC, delayed gadolinium-enhanced MRI of cartilage; ECM, extracellular matrix; FOV, field of view; MAPSS, magnetization-prepared angle-modulated partitioned-*k*-space spoiled gradient echo snapshots; MRI, magnetic resonance imaging; OA, osteoarthritis; PBS, phosphate-buffered saline; PGs, proteoglycans; RF, radiofrequency; ROI, region of interest; SNR, signal-to-noise ratio; $T_{1\rho}$, spin–lattice relaxation in the rotating frame; TE, echo time; TSL, spin-locking time; UTE, ultrashort echo time

Human joints are composed of many different tissues, including articular cartilage, calcified cartilage, menisci, ligaments, tendons and bone, all of which are important to the health of the joint.[10–12] However, conventional spin-locking-prepared MRI pulse sequences are of limited value for the detection of evidence of early PG depletion in deep radial and calcified cartilage, menisci, ligaments and tendons because these tissues typically have T_2 values ranging from submilliseconds to several milliseconds, and thus provide little detectable signal using conventional sequences.[13–15] The lack of signal means that conventional $T_{1\rho}$ sequences are of limited value for the detection of evidence of early biochemical changes, such as PG depletion, in short T_2 tissues. An effective non-invasive assessment of PG depletion could have a major impact in, not only, long T_2 tissues, such as the superficial layer of articular cartilage, but in MR-'invisible' short T_2 tissues, such as deep radial and calcified cartilage, menisci, ligaments and tendons. This, in turn, may improve our ability to make early diagnoses, monitor clinical progress and evaluate new treatments.

In this study, we report the combination of a three-dimensional ultrashort echo time sequence employing Cones trajectories with a self-compensated spin-locking $T_{1\rho}$ preparation (3D UTE-Cones-$T_{1\rho}$) for volumetric $T_{1\rho}$ assessment of short T_2 tissues *in vitro* and *in vivo*. The 3D UTE-Cones sequence has increased signal-to-noise ratio (SNR) efficiency and less sensitivity to eddy currents than the conventional 2D UTE sequence,[16–18] and can potentially provide volumetric assessment of $T_{1\rho}$ values for both short and long T_2 tissues using a clinical 3-T scanner. In this feasibility study, the new sequence was applied to a spherical $CuSO_4$ phantom, *ex vivo* meniscus and tendon samples, as well as knee and ankle joints of healthy volunteers.

2 | METHODS

2.1 | Pulse sequence

All scans were performed on a 3-T Signa Twin Speed scanner (GE Healthcare Technologies, Milwaukee, WI, USA). The sequence consisted of a 3D UTE-Cones sequence preceded by a self-compensated, spin-locking preparation pulse cluster, as shown in Figure 1. The 3D UTE-Cones sequence employed a short radiofrequency (RF)

rectangular pulse (duration, 26–52 μs) for signal excitation, followed by 3D spiral trajectories sampled on the Cones with a minimal nominal TE of 32 μs.[17] The 3D Cones sequence provides volumetric UTE imaging in a time-efficient manner with markedly reduced eddy current artifacts compared with the regular 2D UTE sequence.[19] Furthermore, the 3D Cones sequence has improved SNR efficiency compared with 2D or 3D radial UTE sequences, as 3D spiral trajectories have an improved duty cycle compared with the regular radial trajectories.[20] Moreover, the 3D UTE-Cones sequence allows anisotropic field of view (FOV) and spatial resolution (e.g. higher in-plane resolution and thicker slice), resulting in vastly reduced scan times. This time efficiency greatly benefits clinical applications.

In the 3D UTE-Cones-$T_{1\rho}$ sequence, $T_{1\rho}$ contrast is developed during the spin-locking time (TSL). Quantitative measurement of $T_{1\rho}$ can be achieved by acquiring 3D UTE-Cones-$T_{1\rho}$ images at a series of TSLs. However, this process is time consuming because of the repeated 3D UTE-Cones-$T_{1\rho}$ acquisitions. One approach to reduce the total scan time is to use a relatively short TR (e.g. less than 200 ms). However, this approach may result in significant T_1 contamination because of incomplete recovery of the longitudinal magnetization.[21] T_1 compensation is necessary for accurate measurement of $T_{1\rho}$ based on the following equation[21]:

$$S(TSL) \propto \frac{e^{-TSL/T1\rho} \times (1 - e^{-(TR-TSL)/T1})}{1 - e^{-TSL/T1\rho} \times e^{-(TR-TSL)/T1} \times cos\ \alpha} \times sin\ \alpha + C \qquad (1)$$

where TR is the time between RF excitation pulses with a flip angle α, $T_{1\rho}$ is the spin–lattice relaxation time of the tissue of interest and T_1 is the longitudinal relaxation time of the tissue of interest. A constant term C is introduced to account for background noise and artifacts associated with 3D UTE-Cones-$T_{1\rho}$ data acquisition and image reconstruction. T_1 values of short T_2 tissues can be obtained with 3D Cones data acquisitions with variable TRs.[22] The following equation can be used to fit T_1:

$$S(TR, \alpha) \propto \frac{1 - e^{-TR/T1}}{1 - cos\ \alpha \times e^{-TR/T1}} \times sin\ \alpha + C \qquad (2)$$

where the loss of transverse magnetization during the application of the RF pulse is neglected because of the use of a short rectangular
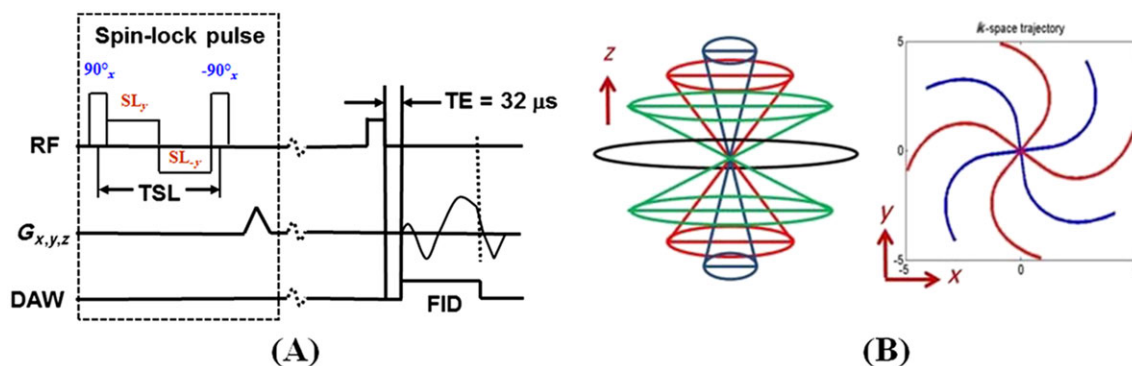

FIGURE 1 Three-dimensional ultrashort echo time cones $T_{1\rho}$ (3D UTE-cones-$T_{1\rho}$) pulse sequence combines a regular 3D UTE cones sequence (minimal nominal TE of 32 μs) with a spin-locking preparation pulse cluster, which consists of a hard 90° pulse, followed by a composition spin-locking pulse and another −90° hard pulse (A). The phase of the second half of the composite spin-locking pulse is shifted 180° from the first half to reduce artifacts caused by B_1 inhomogeneity. The 3D cones sampling trajectory is shown in (B). DAW, data acquisition window; FID, free induction decay; RF, radiofrequency; SL, spin-locking; TE, echo time; TSL, spin-locking time

pulse (duration, 52 μs, 20°). Both longitudinal and transverse relaxations during this short RF pulse are minimal as T_1 values (in the range of hundreds of milliseconds or longer) and T_2^* values (in the range of milliseconds or longer) are much longer than the pulse duration.

Another approach to reduce the total scan time is to acquire multiple spiral spokes (N_{sp}) after each $T_{1\rho}$ preparation. As fat saturation is typically required in $T_{1\rho}$ imaging, N_{sp} Cones trajectory data can be acquired after each fat saturation followed by $T_{1\rho}$ preparation. Up to five spiral spokes were tested in this study. Accuracy was evaluated by comparing the $T_{1\rho}$ values acquired with multiple spiral spokes and the $T_{1\rho}$ values acquired with a single spiral spoke per $T_{1\rho}$ preparation, without and with fat saturation.

2.2 | Simulation

Numerical simulation was performed on a single-component model to fit $T_{1\rho}$ according to Equation 1 and T_1 according to Equation 2. For $T_{1\rho}$ fitting, four images with TSLs of 0.02, 5, 10 and 20 ms were generated with T_1 of 700 ms, $T_{1\rho}$ of 10 ms, TR of 160 ms and a flip angle of 16°. For T_1 fitting, five images with TRs of 6.5, 10, 15, 20 and 30 ms were generated with T_1 of 700 ms and a flip angle of 20°. White noise was added to produce images with SNRs in the range 5–100. For each SNR value, 1000 trials each with different noise realizations were performed using the single-component fitting models described above. The fitted $T_{1\rho}$ and T_1 values, as well as the standard errors as a function of SNR, were analyzed. However, B_1 errors, including B_1 field inhomogeneity and related flip angle errors, were not considered in this study.

2.3 | Phantom, *ex vivo* and *in vivo* studies

We first evaluated the 3D UTE-Cones-$T_{1\rho}$ sequence on a $CuSO_4$ spherical ball phantom using a conventional 2D spiral-$T_{1\rho}$ sequence as reference standard.[6] Then, the 3D UTE-Cones-$T_{1\rho}$ sequence was applied to bovine meniscus samples (n = 4) and human cadaveric Achilles tendon samples (n = 4). Finally, the 3D UTE-Cones-$T_{1\rho}$ sequence was applied to the knee joint of a 28-year-old healthy volunteer and the ankle joint of a 38-year-old healthy volunteer to test the feasibility of this sequence for *in vivo* applications. Institutional Review Board approval and written informed consent were obtained prior to *in vivo* scans. The 3D Cones-$T_{1\rho}$ imaging parameters were as follows: TR = 160 ms; acquisition matrix, 192 × 192; sampling points per Cones spiral trajectory, 380 for the phantom and *in vivo* study and 388 for the *ex vivo* study; sampling duration, 3.04 ms for the phantom and *in vivo* study and 6.21 ms for the ex vivo study; number of Cones spiral trajectories, 5891 for the phantom and in vivo study and 5731 for the *ex vivo* study; number of slices, 30; TE = 32 μs; flip angle, 16°; FOV of 16 cm for the phantom and volunteers and 4 cm for the meniscus and tendon samples; slice thickness, 3 mm for the phantom and volunteers and 1 mm for the meniscus and tendon samples; spin-locking field, 500 Hz; TSL = 0.02/5/10/20 ms for phantom, cartilage and meniscus; TSL = 0.02/1/5/10 ms for tendons. For no fat-saturation imaging, the total scan time was 15 min per TSL. For fat-saturation imaging, five Cones trajectories (N_{sp} = 5) were sampled with each fat saturation and spin-locking preparation pulse, with the same flip angle of 16° and 6–8 ms between acquisitions, and the scan time was reduced to

3 min per TSL. For 2D spiral-$T_{1\rho}$, similar imaging parameters were used with a longer TR of 1500 ms, a longer TE of 5.6 ms for *ex vivo* imaging, sampling points per 2D spiral trajectory of 4096, sampling duration of 16 ms, number of 2D spiral trajectories of 14 and a total scan time of 6 min. A sinc pulse was used for slice-selective excitation in 2D spiral-$T_{1\rho}$ imaging. T_1 effects were minimized by the incorporation of T_1 into the fitting of $T_{1\rho}$. T_1 was measured using 3D Cones data acquisitions with a series of TRs (6.5, 10, 15, 20, 30 ms) and a flip angle of 20° with a total scan time of 7 min. The 2D spiral-$T_{1\rho}$ and 3D UTE-Cones-$T_{1\rho}$ acquisitions without and with fat saturation were applied to phantom and bovine meniscus samples, as well as human Achilles tendon samples. Only 2D spiral-$T_{1\rho}$ and 3D UTE-Cones-$T_{1\rho}$ with fat saturation were applied to healthy human volunteers to save scan time. The samples were stored in phosphate-buffered saline (PBS) solution for 24 h prior to MRI. Each sample was placed in Fomblin solution (Ausimont, Thorofare, NJ, USA), which helped to maintain hydration and minimize susceptibility effects at tissue–air interfaces during MRI. A solenoid coil was used for the meniscus and tendon samples. An eight-channel knee coil was used for the phantom and *in vivo* knee joint study. A quadrature knee coil was used for the *in vivo* Achilles tendon study.

2.4 | Image analysis

SNR was measured for each TSL and was calculated as the ratio of the mean signal intensity inside a user-drawn region of interest (ROI) to the standard deviation of the signal in ROI placed in the background. $T_{1\rho}$ values were obtained using a Levenberg–Marquardt fitting algorithm developed in-house, based on Equation 1. A constant term C was introduced to account for background noise and artifacts associated with UTE data acquisition and image reconstruction. T_1 was quantified through exponential fitting of Equation 2. The analysis algorithm was written in MATLAB (MathWorks Inc., Natick, MA, USA) and was executed offline on axial or sagittal images obtained with the protocols described above. The program allowed the placement of ROIs on the first image of the series, which were then copied to the corresponding position on each of the subsequent images. The mean intensity within each of the ROIs was used for subsequent curve fitting, generating a T_1 or $T_{1\rho}$ value as well as the associated fitting error. Five different regions of interest were fitted to determine the average $T_{1\rho}$ relaxation times and standard deviations for the phantom, meniscus, Achilles tendon and articular cartilage, using a single-component, curve-fitting model.

3 | RESULTS

Numerical simulation studies demonstrated that both $T_{1\rho}$ and T_1 fittings were dependent on the image SNR. With a T_1 of 700 ms, TR of 160 ms, flip angle of 16°, $T_{1\rho}$ of 10 ms and four TSLs ranging from 0.02 to 20 ms, Equation 1 produced errors of <0.01%, 0.4%, 2.5%, 6%, 20.4% and 41.1% in $T_{1\rho}$ fitting with SNRs of 100, 50, 30, 20, 10 and 5, respectively. As the Cones-$T_{1\rho}$ sequence typically generates high-quality images with SNRs of ~45 for menisci in the knee joint and ~20 for the Achilles tendon, the $T_{1\rho}$ fitting error is expected to be in the range 3–6% for *in vivo* studies. A reduced fitting error is

expected for *ex vivo* studies, where the SNR is typically more than 100. With a T_1 of 700 ms, flip angle of 20° and five TRs ranging from 6.5 to 30 ms, Equation 2 produced errors of less than 0.5% with an SNR down to 8, suggesting little fitting error with this model.

The 3D UTE-Cones-$T_{1\rho}$ sequence was successfully implemented for *in vivo* and *ex vivo* studies with negligible artifacts. The $T_{1\rho}$ values obtained from the spherical copper sulfate phantom were about 10% higher with the 3D UTE-Cones-$T_{1\rho}$ sequences (85.7 ± 3.6 ms with N_{sp} = 1 and 89.2 ± 1.4 ms with N_{sp} = 5) than those obtained with the 2D spiral-$T_{1\rho}$ sequence (76.5 ± 1.6 ms), as shown in Figure 2.

Figure 3 shows 3D UTE-Cones-$T_{1\rho}$ imaging of a bovine meniscus. The 2D spiral-$T_{1\rho}$ sequence provided limited signal for the meniscus, whereas the 3D UTE-Cones-$T_{1\rho}$ sequence provided much higher signal with an SNR of 112.5 ± 8.6, which is about six times higher than that of the 2D spiral-$T_{1\rho}$ sequence. A mean T_1 of 638 ± 42 ms was demonstrated for the bovine menisci based on 3D UTE-Cones imaging with a constant flip angle and variable TRs. The 2D spiral-$T_{1\rho}$ of bovine meniscus was reported to be 16.2 ± 0.9 ms, whereas 3D UTE-Cones-$T_{1\rho}$ showed slightly lower values of 10.5 ± 0.8 ms with N_{sp} of 1 and 12.1 ± 0.6 ms with N_{sp} of 5. On average, the four bovine meniscus samples showed a $T_{1\rho}$ of 13.4 ± 1.6 ms with 3D UTE-Cones-$T_{1\rho}$ with fat saturation and N_{sp} of 5, and 18.3 ± 1.8 ms with the 2D spiral-$T_{1\rho}$ sequence.

Figure 4 shows 2D spiral-$T_{1\rho}$ and 3D UTE-Cones-$T_{1\rho}$ imaging of a cadaveric human Achilles tendon sample. A mean T_1 value of 668 ± 34 ms was demonstrated for the human Achilles tendon sample based on 3D UTE-Cones imaging with a constant flip angle and variable TRs. The 2D spiral-$T_{1\rho}$ sequence provided a near-zero signal for the Achilles tendon mainly because of its relatively long TE of 5.6 ms (signal from the Achilles tendon decayed to near zero at this long TE). In comparison, the 3D UTE-Cones-$T_{1\rho}$ sequence provided high signal and spatial resolution for the Achilles tendon sample with an SNR of 25.3 ± 3.8 and $T_{1\rho}$ of 4.0 ± 0.9 ms. On average, the four human Achilles tendon samples showed a $T_{1\rho}$ of 4.3 ± 0.8 ms with 3D UTE-Cones-$T_{1\rho}$ with fat saturation and N_{sp} of 5. $T_{1\rho}$ values were not calculated for any of the human Achilles tendon samples using the 2D spiral-$T_{1\rho}$ sequence because of a lack of signal.

Figure 5 shows 3D UTE-Cones-$T_{1\rho}$ imaging of the knee joint of a 28-year-old healthy male volunteer. Again, the 2D spiral-$T_{1\rho}$ sequence provided limited signal for the meniscus with an SNR of 10.8 ± 2.3, whereas the 3D UTE-Cones-$T_{1\rho}$ sequence provided much higher signal

from the meniscus with an SNR of 44.8 ± 5.2. A mean T_1 of 802 ± 25 ms was demonstrated for the menisci of this volunteer. $T_{1\rho}$ was measured for the tibial plateau articular cartilage (36.1 ± 2.9 ms) and the meniscus (18.3 ± 3.9 ms), as shown in Figure 5B. The $T_{1\rho}$ value derived from the tibial plateau cartilage was about 19% higher (42.8 ± 4.5 ms) with the 2D spiral-$T_{1\rho}$ sequence, consistent with longer T_2 components contributing to spiral-$T_{1\rho}$ imaging.

Figure 6 shows 3D UTE-Cones-$T_{1\rho}$ imaging of the Achilles tendon of a 27-year-old healthy male volunteer. The 2D spiral-$T_{1\rho}$ sequence provided near-zero signal for the Achilles tendon with an SNR of 3.2 ± 0.6, whereas the 3D UTE-Cones-$T_{1\rho}$ sequence provided much higher signal from the Achilles tendon with an SNR of 20.9 ± 3.2. A mean T_1 of 726 ± 43 ms and $T_{1\rho}$ of 3.1 ± 0.4 ms were demonstrated for the Achilles tendon of this volunteer. $T_{1\rho}$ quantification could not be performed on the 2D spiral-$T_{1\rho}$ images because the SNR was too low.

4 | DISCUSSION

There are numerous tissue types comprising the knee joint, including cartilage, ligaments, tendons, synovium, meniscus and bone. Studies have shown that component failures, such as structural changes in collateral ligaments[12] or meniscal damage or position, can lead to cartilage loss.[11,23] For example, Hunter et al.[11] examined the association of meniscal pathological changes with cartilage loss in symptomatic knee OA. They found that each aspect of meniscal abnormality (whether change in position or damage) had a major effect on the risk of cartilage loss.[11] In general, the deterioration or misalignment of any of the tissues comprising the knee joint can increase the progression of OA.[10–12,23] As such, it is essential to be able to image as many components as possible to allow for the comprehensive assessment of longitudinal OA patient groups. UTE provides the ability to image all of the major components in the knee joint,[13,24] and the high signal and coverage afforded by the 3D UTE-Cones sequence indicate that it promises to be a robust solution for this clinical research problem.

In recent years, there has been increased interest in the quantitative imaging of short T_2 tissues, such as tissue components of the knee joint, especially the meniscus.[25–28] For example, Krishnan et al.[25] investigated dGEMRIC imaging of both meniscus and cartilage, and found a significant correlation between T_1(Gd) of the meniscus and
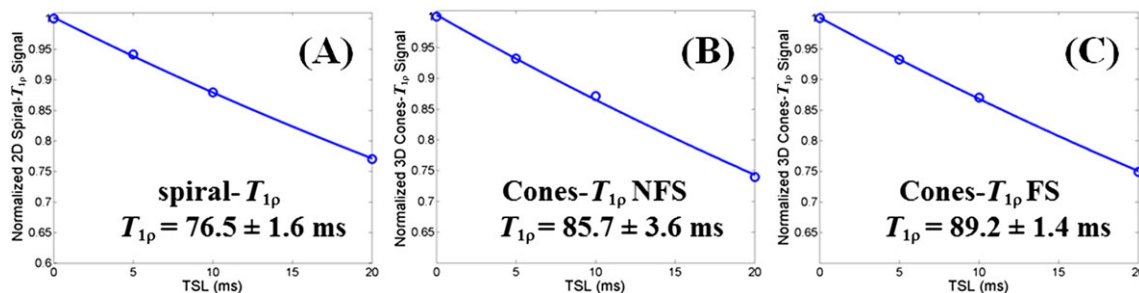

FIGURE 2 $T_{1\rho}$ quantification of a spherical ball phantom filled with copper sulfate using a two-dimensional (2D) spiral-$T_{1\rho}$ sequence, which showed a $T_{1\rho}$ value of 76.5 ± 1.6 ms (a), a three-dimensional ultrashort echo time cones $T_{1\rho}$ (3D UTE-cones-$T_{1\rho}$) sequence, which showed a $T_{1\rho}$ value of 85.7 ± 3.6 ms (B), and a 3D UTE-cones-$T_{1\rho}$ sequence with one spin-locking preparation and one fat saturation pulse followed by five spokes (N_{sp} = 5), which showed a $T_{1\rho}$ value of 89.2 ± 1.4 ms (C). FS, fat saturation; NFS, no fat saturation; TSL, spin-locking time
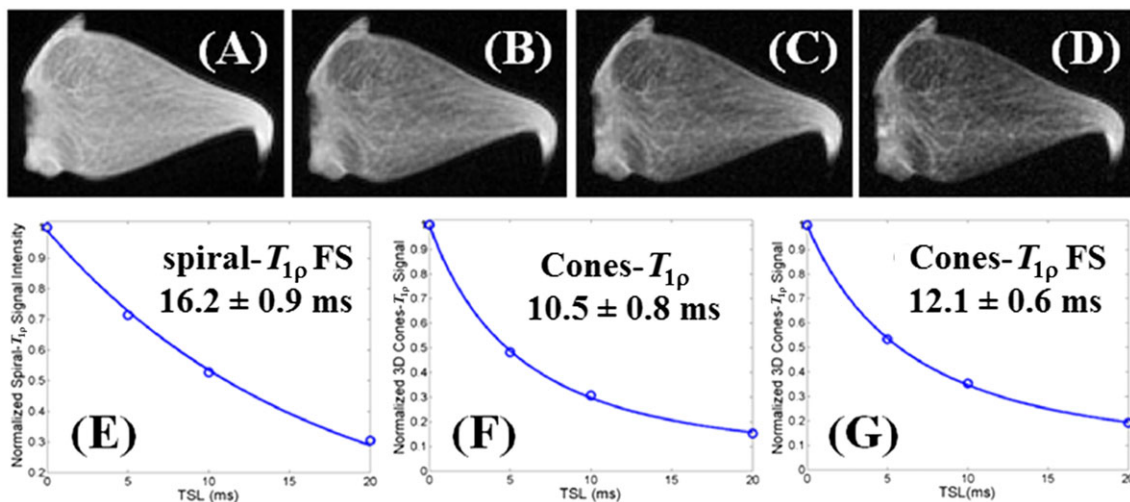
FIGURE 3 Selected three-dimensional ultrashort echo time cones $T_{1\rho}$ (3D UTE-cones-$T_{1\rho}$) images of a bovine meniscus sample with different spin-locking times (TSLs) of 0.02 ms (a), 5 ms (B), 10 ms (C) and 20 ms (D), as well as $T_{1\rho}$ quantification with a two-dimensional (2D) spiral-$T_{1\rho}$ sequence, which showed a $T_{1\rho}$ value of 16.2 ± 0.9 ms (E), 3D cones-$T_{1\rho}$ sequence, which showed a $T_{1\rho}$ value of 10.5 ± 0.8 ms (F), and 3D UTE-cones-$T_{1\rho}$ sequence with one spin-locking preparation and one fat saturation pulse followed by five spokes (N_{sp} = 5), which showed a $T_{1\rho}$ value of 12.1 ± 0.6 ms (G). FS, fat saturation
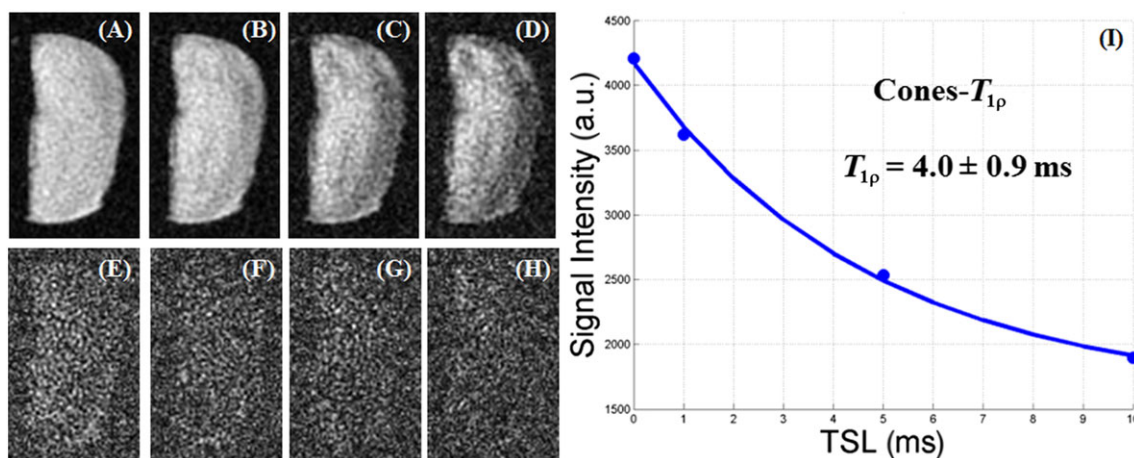

FIGURE 4 Selected three-dimensional ultrashort echo time cones $T_{1\rho}$ (3D UTE-cones-$T_{1\rho}$) images of a cadaveric human Achilles tendon sample with a TE of 32 μs and different spin-locking times (TSLs) of 0.02 ms (a), 1 ms (B), 5 ms (C) and 10 ms (D), as well as spiral-$T_{1\rho}$ imaging of the same sample with a TE of 5.6 ms and different TSLs of 0.02 ms (E), 1 ms (F), 5 ms (G) and 10 ms (H). $T_{1\rho}$ of the Achilles tendon sample can only be quantified with the 3D UTE-cones-$T_{1\rho}$ sequence, which showed a $T_{1\rho}$ value of 4.0 ± 0.9 ms (I)

T_1(Gd) of the articular cartilage of the knee in OA. These interesting results suggest that knee joint degeneration occurs in both tissues.[25] Rauscher et al.[26] reported a high correlation between meniscal $T_{1\rho}$ and clinical findings of OA, suggesting the importance of $T_{1\rho}$ imaging of the meniscus. Bolbos et al.[27] investigated the relationship between meniscal $T_{1\rho}$ and adjacent cartilage $T_{1\rho}$ in knees with acute anterior cruciate ligament injuries, and found a strong injury-related relationship between meniscus and cartilage biochemical changes. Wang et al.[28] investigated the subregional, compartmental and whole $T_{1\rho}$ values of menisci in patients with doubtful/minimal relative to moderate/severe OA and healthy controls at 3 T. They found that lateral anterior and medial posterior meniscus subregions in healthy controls showed significantly lower $T_{1\rho}$ values than the corresponding meniscus subregions in patients with OA. These results suggest that damage in the medial posterior subregion and medial compartment of menisci

might be associated with OA.[28] A drawback of the above techniques is that they all utilized clinical gradient echo sequences with a TE of around 4 ms, which is comparable to the T_2^* value of the meniscus and is therefore too long to detect the short T_2 components that comprise a significant proportion of the entire tissue. The long T_2 components in the meniscus were probably the only contribution to the detected signal. UTE-type sequences, with much shorter TEs, are expected to provide better depiction and characterization of the meniscus. Therefore, the 3D UTE-Cones-$T_{1\rho}$ sequence is likely to provide more accurate assessment of PGs in the meniscus relative to the $T_{1\rho}$ sequence based on conventional gradient echo sequences.[26–28]

By definition, the TEs of UTE sequences are very short and the ability to reduce TR to decrease the imaging time is promising. The complication of reducing TR is the reduced recovery of the longitudinal magnetization. At steady state, this introduces T_1 contamination, as
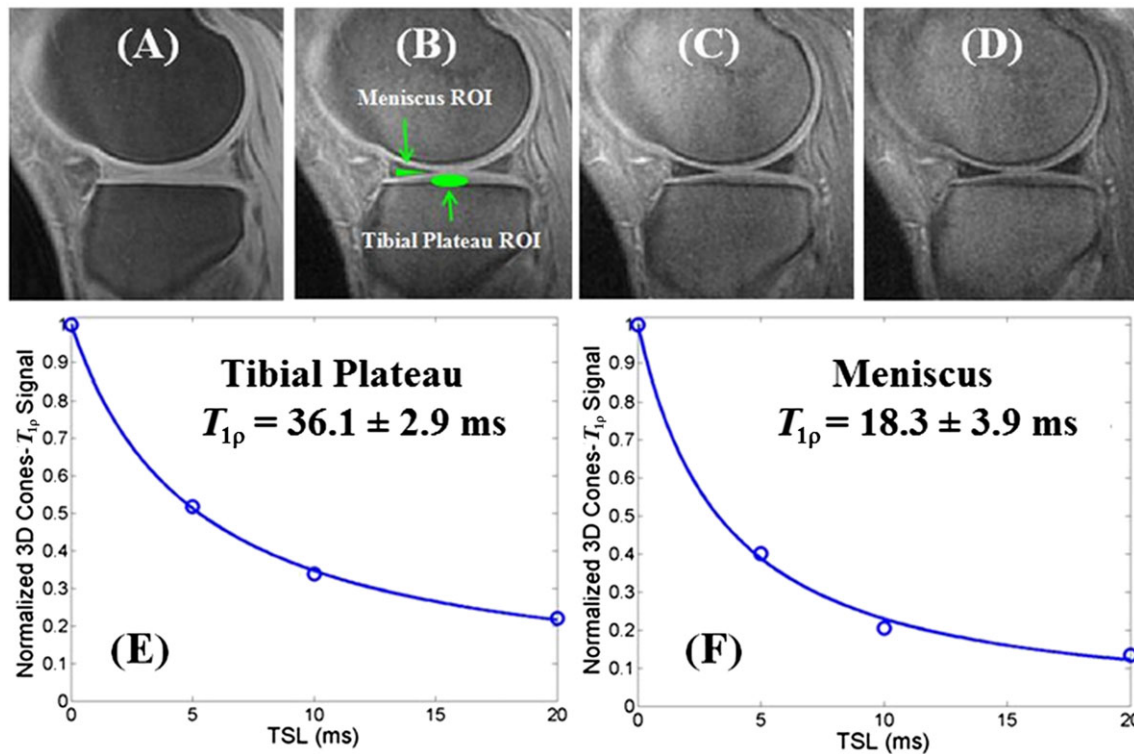
FIGURE 5 Selected three-dimensional ultrashort echo time cones $T_{1\rho}$ (3D UTE-cones-$T_{1\rho}$) images of the knee joint of a 28-year-old healthy male volunteer with four different spin-locking times (TSLs) of 0.02 ms (a), 5 ms (B), 10 ms (C) and 20 ms (D). The femorotibial cartilage and meniscus are seen with high spatial resolution, signal and contrast. Single-component curve fitting shows a $T_{1\rho}$ value of 36.1 ± 2.9 ms for the articular cartilage (E) and 18.3 ± 3.9 ms for the meniscus (F). ROI, region of interest
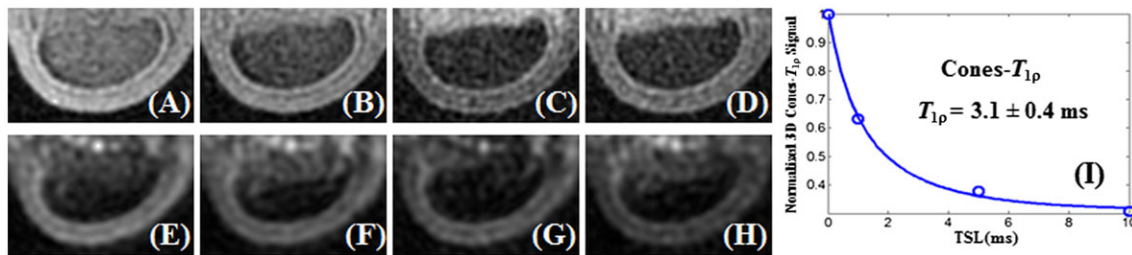

FIGURE 6 The Achilles tendon of a 38-year-old healthy male volunteer imaged using the three-dimensional ultrashort echo time cones $T_{1\rho}$ (3D UTE-cones-$T_{1\rho}$) sequence with four different spin-locking times (TSLs) of 0.02 ms (a), 1 ms (B), 5 ms (C) and 10 ms (D), and the two-dimensional (2D) spiral-T1ρ sequence with four different TSLs of 0 ms (E), 1 ms (F), 5 ms (G) and 10 ms (H). The Achilles tendon was depicted with high spatial resolution, signal and contrast with the 3D UTE-cones-T1ρ sequence, but with near-zero signal with the 2D spiral-$T_{1\rho}$ sequence. Single-component curve fitting shows a $T_{1\rho}$ value of 3.1 ± 0.4 ms for the Achilles tendon, which could only be measured with the 3D UTE-cones-$T_{1\rho}$ sequence (I)

described by Aronen et al.[21] The ability to accurately report and compare $T_{1\rho}$ values across different pulse sequences and field strengths is important. To accurately account for T_1 contamination, T_2^* and T_1 values of the tissue are required,[29] resulting in increased scan time. This compensation is further confounded by multiple components of T_2^* relaxation commonly encountered in UTE musculoskeletal applications,[30–32] which limits comparisons with $T_{1\rho}$ sequences based on conventional clinical sequences with much longer TEs.[4–6]

We employed Cones acquisitions with variable TRs for efficient volumetric T_1 mapping. The Cones acquisition is important, especially for short T_2 tissues whose T_1 values cannot be readily measured with conventional clinical techniques.[22] However, this technique is sensitive to flip angle errors. Cones imaging with actual flip angle imaging is one

method for accurate T_1 mapping of short T_2 tissues,[33,34] and will be investigated in future studies. Another approach used to reduce the total scan time is to acquire multiple spokes per spin-locking preparation and fat saturation. This approach markedly reduced the total scan time by N_{sp}, but affected only moderately the $T_{1\rho}$ values, as demonstrated in the phantom and bovine meniscus sample studies shown in Figures 2 and 3, respectively.

The 3D UTE-Cones-$T_{1\rho}$ sequence is expected to provide lower $T_{1\rho}$ values for short T_2 tissues, such as menisci and tendons, because of the contribution of the shorter T_2 components, which may be detected with the 3D UTE-Cones-$T_{1\rho}$ sequence with a TE value of 32 μs, but is difficult to detect with conventional gradient echo-based $T_{1\rho}$ sequences with much longer TEs.[26–28] For example, Wang et al.[28]

applied a 3D gradient echo-based $T_{1\rho}$ sequence to the knee and reported a $T_{1\rho}$ value of around 28 ms for healthy menisci, which is about 56% longer than the $T_{1\rho}$ value measured with the 3D UTE-Cones-$T_{1\rho}$ sequence. However, shorter $T_{1\rho}$ values were found for the menisci of healthy volunteers by Rauscher et al.,[26] who reported a $T_{1\rho}$ value of around 14.7 ms (a TE value of 4.1 ms was used), and by Bolbos et al.,[27] who reported a $T_{1\rho}$ value of around 15 ms (a TE value of 3.7 ms was used). Clearly, more research is needed to clarify this discrepancy. The Achilles tendon is 'invisible' with all conventional clinical sequences, and its $T_{1\rho}$ value cannot be assessed with conventional $T_{1\rho}$ sequences. The UTE-based $T_{1\rho}$ sequence seems to be a good approach for reliable $T_{1\rho}$ measurement of this tissue with extremely short T_2^* values (typically less than 2 ms),[14] as demonstrated in Figures 3 and 6. Furthermore, it is likely that there is a bi-component $T_{1\rho}$ contribution from short and long T_2 components of meniscus and Achilles tendon, as well as other short T_2 tissues. Bi-component $T_{1\rho}$ analysis would require more TSLs and longer scan times, which makes clinical implementation challenging, and therefore more research on acceleration is needed.

There are several limitations of this study. First, only technical feasibility is shown in this study. The bovine meniscus seems to have a longer $T_{1\rho}$ value than the human meniscus (18 *versus* 10 ms), and *ex vivo* human Achilles tendon seems to have a longer $T_{1\rho}$ value than the *in vivo* human Achilles tendon (4 *versus* 3 ms). Further research is needed to correlate Cones-$T_{1\rho}$ with tissue degeneration. The application to patients with OA remains to be investigated. Second, the UTE-Cones-$T_{1\rho}$ sequence employs 3D spiral data sampling, which may generate spatially varying spiral artifacts and thus affect noise calculation, leading to errors in $T_{1\rho}$ fitting. However, this error is likely to be small considering the high SNR of 3D UTE-Cones-$T_{1\rho}$ images. Third, T_1 errors as a result of B_1 inhomogeneity are not considered in this study and will be investigated in the future.[33,34] Fourth, fat saturation is less effective when multiple spiral spokes are acquired following each fat saturation and spin-lock preparation. Residual signal from bone marrow fat may infiltrate into the adjacent deep layer of articular cartilage or other soft tissues as a result of an off-resonance effect, resulting in quantification error. Fifth, a long T_2 phantom was used in this study without further validation on short T_2 phantoms. This is because the reference 2D spiral $T_{1\rho}$ sequence has a minimal TE of >3 ms and cannot reliably evaluate short T_2 phantoms. Sixth, multiple spiral spokes are sampled after each spin-locking preparation. Although this approach greatly reduces the total scan time, it also leads to an overestimation of $T_{1\rho}$ by about 4%. This error is likely to be a result of different $T_{1\rho}$ contrast for each spiral interleave as each spiral trajectory goes through the k-space center, and each of the five spiral trajectories has different T_1 relaxation. The 3D magnetization-prepared angle-modulated partitioned-k-space spoiled gradient echo snapshots (3D MAPSS) sequence employs a similar approach by acquiring multiple Cartesian k-space lines of data per spin-locking preparation.[35] However, in 3D MAPSS, most of the Cartesian lines do not pass through the k-space center, and thus the difference in T_1 relaxation for these data does not affect $T_{1\rho}$ calculation.

Our study demonstrates the feasibility of $T_{1\rho}$ imaging of short T_2 tissues, such as meniscus and Achilles tendon, with the 3D UTE-Cones-$T_{1\rho}$ sequence. The self-compensated, spin-locking preparation pulse preceding the 3D Cones sequence provides a novel SNR-efficient method to obtain volumetric $T_{1\rho}$ contrast in a clinically accessible scan time. In addition to increased volumetric coverage (relative to 2D radial UTE imaging), the reduced artifacts and increased signal should provide improved reliability for longitudinal studies validating UTE $T_{1\rho}$ for the assessment of OA progression.

REFERENCES

1. Grushko G, Schneiderman R, Maroudas A. Some biochemical and biophysical parameters for the study of the pathogenesis of osteoarthritis: A comparison between the processes of aging and degeneration in human hip cartilage. *Connect Tissue Res.* 1989;19:149-176.

2. Bashir A, Gray ML, Burstein D. Gd-DTPA^{2-} as a measure of cartilage degradation. *Magn Reson Med.* 1996;36:665-673.

3. Shapiro EM, Borthakur A, Gougoutas A, Reddy R. ^{23}Na MRI accurately measures fixed charge density in articular cartilage. *Magn Reson Med.* 2002;47:284-291.

4. Duvvuri U, Reddy R, Patel SD, Kaufman JH, Kneeland JB, Leigh JS. T1rho-relaxation in articular cartilage: Effects of enzymatic degradation. *Magn Reson Med.* 1997;38:863-867.

5. Regatte RR, Akella SVS, Lonner JH, Kneeland JB, Reddy R. T1ρ relaxation mapping in human osteoarthritis (OA) cartilage: Comparison of T1ρ with T2. *J Magn Reson Imaging.* 2006;23:547-553.

6. Li X, Han ET, Ma B, Link TM, Newitt DC, Majumdar S. In vivo 3 T spiral imaging based multi-slice T1ρ mapping of knee cartilage in osteoarthritis. *Magn Reson Med.* 2005;54:929-936.

7. Knispel RR, Thompson RT, Pintar MM. Dispersion of proton spin–lattice relaxation in tissues. *J Magn Reson.* 1974;14:44-51.

8. Duvvuri U, Charagundla SR, Kudchodkar SB, et al. Human knee: In vivo T1ρ-weighted MR imaging at 1.5 T – Preliminary experience. *Radiology.* 2001;220:822-826.

9. Li X, Ma B, Link TM, et al. In vivo T1ρ and T2 mapping of articular cartilage in osteoarthritis of the knee using 3 T MRI. *Osteoarthritis Cartilage.* 2007;15:789-797.

10. Brandt KD, Radin EL, Dieppe PA, Putte L. Yet more evidence that osteoarthritis is not a cartilage disease (editorial). *Ann Rheum Dis.* 2006;65:1261-1264.

11. Hunter DJ, Zhang YQ, Niu JB, et al. The association of meniscal pathologic changes with cartilage loss in symptomatic knee osteoarthritis. *Arthritis Rheum.* 2006;54:795-801.

12. Tan AL, Toumi H, Benjamin M, et al. Combined high-resolution magnetic resonance imaging and histological examination to explore the role of ligaments and tendons in the phenotypic expression of early hand osteoarthritis. *Ann Rheum Dis.* 2006;65:1267-1272.

13. Chang EY, Du J, Bae WC, Chung CB. Qualitative and quantitative ultrashort echo time imaging of musculoskeletal tissues. *Semin Musculoskelet Radiol.* 2015;19(4):375-386.

14. Du J, Carl M, Diaz E, et al. Ultrashort TE T1rho (UTE T1rho) imaging of the Achilles tendon and meniscus. *Magn Reson Med.* 2010;64(3):834-842.

15. Du J, Carl M, Bae WC, et al. Dual inversion recovery ultrashort echo time (DIR-UTE) imaging and quantification of the zone of calcified cartilage (ZCC). *Osteoarthritis Cartilage.* 2013;21(1):77-85.

16. Gurney PT, Hargreaves BA, Nishimura DG. Design and analysis of a practical 3D cones trajectory. *Magn Reson Med.* 2006;55(3):575-582.

17. Carl M, Bydder GM, Du J. UTE imaging with simultaneous water and fat signal suppression using a time-efficient multispoke inversion recovery pulse sequence. *Magn Reson Med*. 2016;76:577-582.

18. Lu A, Daniel BL, Pauly JM, Pauly KB. Improved slice selection for R2* mapping during cryoablation with eddy current compensation. *J Magn Reson Imaging*. 2008;28:190-198.

19. Gatehouse PD, Bydder GM. Magnetic resonance imaging of short T2 components in tissue. *Clin Radiol*. 2003;58:1-19.

20. Tsai CM, Nishimura DG. Reduced aliasing artifacts using variable-density k-space sampling trajectories. *Magn Reson Med*. 2000;43:452-458.

21. Aronen HJ, Peltonen TK, Tanttu JI, et al. Spin-lock imaging in contrast-enhanced magnetic resonance imaging of human gliomas. *Acad Radiol*. 1996;3(Suppl 2):S170-S172.

22. Chen J, Chang EY, Carl M, et al. Quantification of bound and pore water T1 relaxation times in cortical bone using three-dimensional ultrashort echo time (3D UTE cones) sequences. *Magn Reson Med*. 2016; Jun 6 (Epub ahead of print)

23. Hunter DJ, Zhang Y, Niu J, et al. Structural factors associated with malalignment in knee osteoarthritis: The Boston osteoarthritis knee study. *J Rheumatol*. 2005;32(11):2192-2199.

24. Williams A, Qian Y, Chu CR. Assessing degeneration of human articular cartilage with ultra-short echo time (UTE) T2* mapping. *Osteoarthritis Cartilage*. 2010;18:539-546.

25. Krishnan N, Shetty SK, Williams A, Mikulis B, McKenzie C, Burstein D. Delayed gadolinium-enhanced magnetic resonance imaging of the meniscus: An index of meniscal tissue degeneration? *Arthritis Rheum*. 2007;56(5):1507-1511.

26. Rauscher I, Stahl R, Cheng J, et al. Meniscal measurements of T1rho and T2 at MR imaging in healthy subjects and patients with osteoarthritis. *Radiology*. 2008;249(2):591-600.

27. Bolbos RI, Link TM, Ma CB, Majumdar S, Li X. T1rho relaxation time of the meniscus and its relationship with T1rho of adjacent cartilage in knees with acute ACL injuries at 3 T. *Osteoarthritis Cartilage*. 2009;17(1):12-18.

28. Wang L, Chang G, Bencardino J, et al. T1rho MRI of menisci in patients with osteoarthritis at 3 Tesla: A preliminary study. *J Magn Reson Imaging*. 2014;40(3):588-595.

29. Chen W. Errors in quantitaive t1rho imaging and the correction methods. *Quant Imaging Med Surg*. 2015;5:583-591.

30. Qian Y, Williams AA, Chu CR, Boada FE. Multicompartment T2* mapping of knee cartilage: Technical feasibility ex vivo. *Magn Reson Med*. 2010;64:1427-1432.

31. Du J, Diaz E, Carl M, Bae W, Chung CB, Bydder GM. Ultrashort TE (UTE) imaging with bi-component analysis. *Magn Reson Med*. 2012;67:645-649.

32. Diaz E, Chung CB, Bae W, et al. Ultrashort TE spectroscopic imaging (UTESI): An efficient method for quantifying bound and free water. *NMR Biomed*. 2012;25:161-168.

33. Yarnykh V. Actual flip-angle imaging in the pulsed steady state: A method for rapid three-dimensional mapping of the transmitted radio-frequency field. *Magn Reson Med*. 2006;57:192-200.

34. Han M, Larson P, Krug R, Rieke V. Actual flip angle imaging to improve T1 measurement for short T2 tissues. *Proceedings of the 23rd Annual Meeting ISMRM*, Toronto, ON, Canada, June 2015; P501.

35. Li X, Han ET, Ma B, Busse RF, Majumdar S. In vivo T1ρ mapping in cartilage using 3D magnetization-prepared angle-modulated partitioned k-space spoiled gradient echo snapshots (3D MAPPS). *Magn Reson Med*. 2008;59:298-307.